



1 **Eco-evolutionary Modelling of Global Vegetation Dynamics and the Impact of CO₂**
2 **during the late Quaternary: Insights from Contrasting Periods**

3 Jierong Zhao¹, Boya Zhou², Sandy P. Harrison^{1,*}, Iain Colin Prentice²

4 ¹ Department of Geography and Environmental Science, University of Reading, Whiteknights,
5 Reading, RG6 6AB, UK

6 ² Georgina Mace Centre for the Living Planet, Department of Life Sciences, Imperial College
7 London, Silwood Park Campus, Buckhurst Road, Ascot, SL5 7PY, UK

8 * Corresponding author: s.p.harrison@reading.ac.uk

9

10 **Abstract**

11 Changes in climate have had major impacts on global vegetation during the Quaternary.
12 However, variations in CO₂ levels also play a role in shaping vegetation dynamics by
13 influencing plant productivity and water-use efficiency, and consequently the relative
14 competitive success of the C₃ and C₄ photosynthetic pathways. We use an eco-evolutionary
15 optimality (EEO) based modelling approach to examine the impacts of climate fluctuations and
16 CO₂-induced alterations on gross primary production (GPP). We considered two contrasting
17 periods, the Last Glacial Maximum (LGM, 21,000 years before present) and the mid-Holocene
18 (MH, 6,000 years before present) and compared both to pre-industrial conditions (PI). The
19 LGM, characterised by generally colder and drier climate, had a CO₂ level close to the
20 minimum for effective C₃ plant operation. In contrast, the MH had warmer summers and
21 increased monsoonal rainfall in the northern hemisphere, although with a CO₂ level still below
22 PI. We simulated vegetation primary production at the LGM and the MH compared to the PI
23 baseline using a light-use efficiency model that simulates GPP coupled to an EEO model that
24 simulates leaf area index (LAI) and C₃/C₄ competition. We found that low CO₂ at the LGM
25 was nearly as important as climate in reducing tree cover, increasing the abundance of C₄ plants
26 and lowering GPP. Global GPP in the MH was similar to the PI (although greater than the
27 LGM), also reflecting CO₂ constraints on plant growth despite the positive impacts of warmer
28 and/or wetter climates experienced in the northern hemisphere and tropical regions. These
29 results emphasise the importance of taking account of impacts of changing CO₂ levels on plant
30 growth to model ecosystem changes.
31



32 **1 Introduction**

33 Vegetation regulates the exchanges of energy, water, and carbon dioxide between the land and
34 the atmosphere (Williams and Torn, 2015; Forzieri et al., 2020; Hoek van Dijke et al., 2020).
35 Gross primary production (GPP), defined as the carbon uptake by vegetation through
36 photosynthesis at the ecosystem scale, determines the extent to which the terrestrial biosphere
37 can mitigate CO₂ emissions (Bonan, 2008; Zeng et al., 2017; Chen et al., 2019). There is a tight
38 coupling between CO₂ uptake and water loss via stomata, such that when ambient CO₂ is high
39 water-use efficiency (the amount of water required for transpiration to achieve a unit of CO₂
40 assimilation) is also high (Medlyn et al., 2017). Recent global greening trends are thought to
41 reflect both changes in climate, particularly warming at high latitudes, and the effect of
42 increasing CO₂ on water-use efficiency (Cai and Prentice, 2020; Piao et al., 2020). However,
43 there is still uncertainty about the relative importance of these two effects on recent changes in
44 global GPP, in part because recent climate changes have been largely driven by the increase in
45 CO₂.

46 Past climate states provide opportunities to examine the role of climate and CO₂ in modulating
47 GPP when there is a greater de-coupling between changes in CO₂ and climate. The contrast
48 between glacial and interglacial states during the Late Quaternary offers an ideal opportunity
49 to separate the impact of these two factors on vegetation. Glacial-interglacial shifts in climate
50 are largely driven by changes in orbital configuration which resulted in changes in the seasonal
51 and latitudinal patterns of incoming solar radiation (Berger, 1978; Berger and Loutre, 1991).
52 The Last Glacial Maximum (LGM), ca 21,000 years ago, had an orbital configuration similar
53 to the present but was characterised by the presence of large continental ice sheets and generally
54 colder and drier climates (Kageyama et al., 2021). The CO₂ level was ca 190 ppm, which is
55 close to the minimum for effective C₃ plant operation (Gerhart and Ward, 2010). The mid-
56 Holocene (MH), ca 6000 years ago, was characterised by a significantly different seasonal and
57 latitudinal distribution of incoming solar radiation (a result of changes in obliquity and
58 precession) which affected light availability for photosynthesis and produced warmer summers
59 in the northern hemisphere and wetter conditions in the sub-tropics (Brierley et al., 2020).
60 However, ambient CO₂ was only ca 264 ppm (Otto-Bleisner et al., 2017), somewhat lower than
61 the pre-industrial (PI) period (285 ppm) and considerably lower than today.

62 Previous work on the impact of low CO₂ on vegetation at the LGM has focused mainly on the
63 implications for tree cover (e.g. Harrison and Prentice, 2003; Prentice et al., 2011; Bragg et al.,
64 2013; Martin Calvo and Prentice, 2015) rather than vegetation productivity. There has been
65 work on the implications of MH climate for vegetation patterns (e.g. Kaplan et al., 2003;
66 Wohlfahrt et al., 2008), but there has been little consideration of the impact of climate and CO₂
67 on overall productivity during this period. The role of changes in solar radiation for
68 photosynthesis has not been examined in either period. In this study, we use an eco-
69 evolutionary optimality (EEO) based modelling approach to investigate the relative importance
70 of climate, solar radiation and CO₂ changes on the respective contributions of C₃ and C₄ plants
71 to total GPP, focusing on the LGM and MH states compared to a pre-industrial baseline. We
72 use a series of counter-factual experiments to examine the magnitude of changes due to
73 individual drivers (climate parameters, solar radiation and CO₂) on the simulated GPP and to
74 determine the regions where specific factors are most influential.



75 **2 Methods**

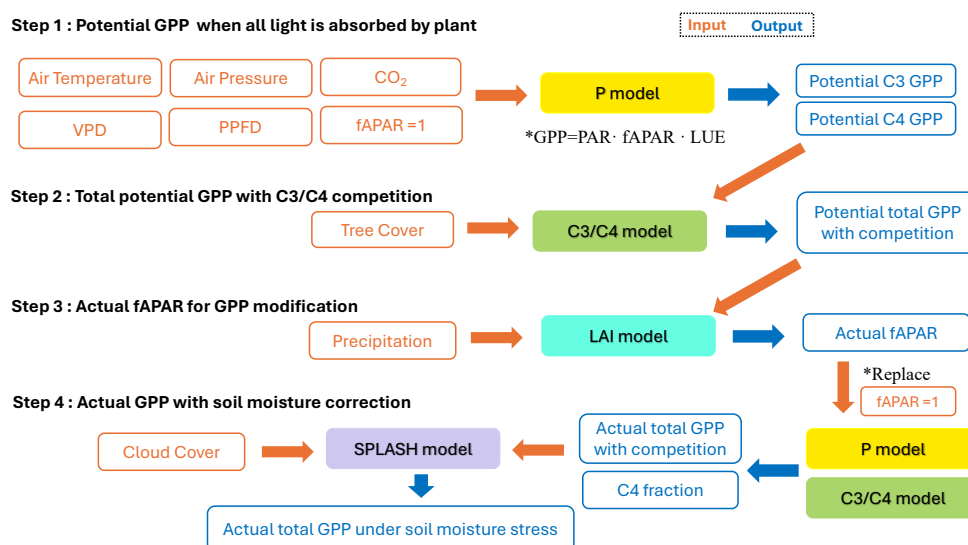
76

77 **2.1 Modelling Scheme**

78 We simulated vegetation changes at the LGM and the MH compared to the pre-industrial (PI)
 79 state using a sequence of linked models that predict GPP, leaf area index (LAI) and C₃/C₄
 80 competition based on EEO theory (Fig. 1).

81 The P model (Wang et al., 2017, Stocker et al., 2020) is a light-use efficiency model that
 82 simulates GPP. It uses the Farquhar-von Caemmerer-Berry photosynthesis model (Farquhar et
 83 al., 1980) for instantaneous biochemical processes combined with two EEO hypotheses
 84 describing photosynthetic acclimation, the ‘coordination’ and ‘least- cost’ hypotheses (Prentice
 85 et al., 2014, Wang et al., 2017), to account for the spatial and temporal acclimation of
 86 carboxylation and stomatal conductance to environmental variations at weekly to monthly time
 87 scales. Although the P model simulates both C₃ and C₄ photosynthesis, it does not need to make
 88 any other distinctions between plant functional types. The required inputs to the model (Fig. 1)
 89 are air temperature (°C), vapour pressure deficit (VPD, Pa) derived from relative humidity, air
 90 pressure (Pa) (to account for the effect of elevation on photosynthesis, incident photosynthetic
 91 photon flux density (PPFD, $\mu\text{mol m}^{-2} \text{s}^{-1}$) estimated from short wave solar radiation, and
 92 ambient CO₂ concentration. The P model has been extensively validated and shown to predict
 93 the geographic patterns of GPP under modern conditions successfully (Wang et al., 2017;
 94 Stocker et al., 2020). Furthermore, it correctly predicts related physiological characteristics,
 95 including the global pattern of the maximum carboxylation (V_{cmax}) rate in relation to gradients
 96 in PPFD, temperature and VPD (Smith et al., 2019), the seasonal variation of V_{cmax} in different
 97 biomes (Jiang et al., 2020), its response to atmospheric CO₂ (Smith and Keenan, 2020), and
 98 the variation of photosynthetic traits along elevational gradients (Peng et al., 2020).

99



100

101

102

103

Figure 1: Flowchart showing the steps in the modelling procedure.



104 The P model simulates potential GPP for C₃ and C₄ plants separately (Figure 1). These
105 estimates were fed into a simple model of C₃/C₄ competition based on the P model (Lavergne
106 et al., 2024). The relative advantage of C₄ plants is estimated as the difference between the
107 monthly potential GPP for C₃ and C₄ plants, summed over the year. The C₄ share of total GPP
108 was then estimated by fitting a logistic curve between the model estimated C₄ relative
109 advantage and observed C₄ abundance. These calculations assume that neither water nor
110 nutrients are limiting growth. However, under these conditions, C₃ trees out-compete C₄
111 grasses through shading, even where the C₄ pathway would yield higher rates of
112 photosynthesis. The model accounts for this using an additional function relating the proportion
113 of GPP from trees to total potential GPP based on a power function for the relationship between
114 prescribed annual mean percentage tree cover and the simulated annual GPP of C₃ plants. Thus,
115 tree cover is an additional required input to the competition model (Figure 1). The competition
116 model also uses a minimum temperature threshold to define conditions under which C₄ plants
117 cannot grow, where this limit is set to a minimum temperature of the coldest month of -24°
118 based on experimental data. The competition model has been shown to reproduce global
119 patterns in the relative abundance of C₃/C₄ plants as well as the observed rate of $\Delta^{13}\text{C}$ in recent
120 decades, as shown by independent atmospheric estimates (Lavergne et al., 2020).

121 To convert potential GPP to actual GPP, we used an LAI model (Figure 1) that predicts the
122 seasonal cycle of LAI based on environmental conditions and an estimate of the potential GPP,
123 i.e. the GPP predicted when the fraction of absorbed photosynthetically active radiation,
124 fAPAR, is set to 1 (Zhou et al., 2024). The seasonal LAI is calculated using a moving average
125 to represent the time lag between allocation to leaves and modelled steady-state LAI. A
126 seasonal maximum fAPAR model was embedded in this model to limit seasonal LAI
127 predictions (Zhu et al., 2022; Cai et al., 2023). The calculation of seasonal maximum fAPAR
128 incorporates a water-carbon trade-off: it is defined as the lesser of an energy-limited
129 (maximising GPP) and a water-limited (maximising the use of available precipitation) estimate
130 (Zhu et al., 2022; Cai et al., 2023). The seasonal LAI is calculated using a moving average to
131 represent the time lag between allocation to leaves and modelled steady-state LAI. The model
132 has been shown to capture LAI dynamics across biomes, both at individual eddy-covariance
133 flux measurement sites and spatial patterns (Zhou et al., 2024). The seasonal cycle of fAPAR
134 is calculated from the seasonal cycle of LAI using Beer's law (Swinehart, 1962) and this is
135 then used to calculate seasonal changes in actual GPP. Finally, we apply an empirical soil
136 moisture correction ($\beta(\theta)$: Stocker et al., 2020) to account for the impact of soil moisture stress
137 on GPP, using the Simple Process-Led Algorithms for Simulating Habitats (SPLASH) model
138 (Davis et al., 2017).

139 2.2. Derivation of LGM, MH and PI climate inputs

140 We use LGM, MH and pre-industrial (PI) climate simulations run using the low-resolution
141 version of the Max Planck Institute Earth System Model (MPI-ESM1.2-LR; Mauritsen et al.,
142 2019; doi:10.22033/ESGF/CMIP6.6642) made as part of the fourth phase of the Palaeoclimate
143 Modelling Intercomparison Project (PMIP4; Kageyama et al., 2017; Otto-Bleisner et al., 2019).
144 This model is amongst the best performing of the PMIP models when evaluated using
145 reconstructions of land and ocean climates (Brierley et al., 2020; Kageyama et al., 2021) and
146 uniquely has archived all the necessary outputs needed to run the EEO-based models (Fig. 1).
147 The experiments were run following the PMIP4 protocols for each time period (Kageyama et
148 al., 2017; Otto-Bleisner et al., 2019). The PI experiment was run for 1000 years using modern
149 ice sheet and land-sea configurations and a CO₂ level of 284.3 ppm (SI Table 1). The MH
150 experiment uses the same ice sheet and land-sea configurations as the PI but uses appropriate



151 changes in orbital parameters and a CO₂ level of 264.4 ppm (SI Table 1). The MPI-ESM1.2-
152 LR LGM experiment uses the ICE6G_C ice sheet and corresponding modification in land-sea
153 geography, appropriate orbital parameters and a CO₂ level of 190 ppm (SI Table 1). The LGM
154 simulation was re-started from a previous LGM simulation and then spun-up for 3850 years.

155 The MPI-ESM1.2-LR model has a spectral resolution of T63 (192 x 96 longitude/latitude). The
156 outputs necessary to run the EEO-based models were down-scaled to a resolution of 0.5° using
157 spline interpolation. The daily data necessary to run the EEO-based models was obtained from
158 monthly data, also using nearest neighbour and bilinear interpolation. Although many previous
159 vegetation modelling studies have used climate anomalies from a baseline experiment (e.g.
160 LGM minus PI), here we used model outputs directly – because although the anomaly approach
161 is well-suited to adjust climate variables, it cannot be used to adjust simulated tree cover.

162 2.3. Stein-Alpert decomposition

163 Climate, light availability and atmospheric CO₂ concentration have independent effects on
164 plant growth. To evaluate the unique effects of these different factors, and potential synergies
165 between them, on the changes in GPP between the PI and the LGM and MH experiments, we
166 used the Stein-Alpert decomposition method (Stein and Alpert, 1993), an approach that has
167 been previously shown to be useful in evaluating the impacts of different factors on past
168 vegetation changes (e.g. Martin-Calvo and Prentice, 2015; Sato et al., 2021). We used the pre-
169 industrial simulation as the reference case (f₀) and ran a series of factorial experiments in which
170 specific factors were changed to their LGM or MH conditions as follows:

- 171
172 Experiment f1: LGM (or MH) climate, PI CO₂ and PPF
173 Experiment f2: LGM (or MH) CO₂, PI climate and PPF
174 Experiment f3: LGM (or MH) PPF, PI climate and CO₂
175 Experiment f12: LGM (or MH) climate and CO₂, PI PPF
176 Experiment f13: LGM (or MH) climate and PPF, PI CO₂
177 Experiment f23: LGM (or MH) CO₂ and PPF, PI climate
178 Experiment f123: LGM (or MH) climate, CO₂ and PPF
179

180 The impact of each factor or combination of factors was then calculated as:

181
182 $\langle f1 \rangle = f1 - f0$
183 $\langle f2 \rangle = f2 - f0$
184 $\langle f3 \rangle = f3 - f0$
185 $\langle f12 \rangle = f12 - (f1 + f2) + f0$
186 $\langle f13 \rangle = f13 - (f1 + f3) + f0$
187 $\langle f23 \rangle = f23 - (f2 + f3) + f0$
188 $\langle f123 \rangle = f123 - (f12 + f13 + f23) + (f1 + f2 + f3) - f0$
189

190 where the first three experiments represent the influence of the single changed factor, the
191 second three experiments represent synergies between pairs of factors, and the final experiment
192 represents the three-way synergy between all three factors.

193 The comparisons can only be made for the common land area between the PI and each
194 palaeoclimate experiment. The LGM factorial experiments therefore have a baseline GPP value
195 for the f₀ experiment that does not include the areas exposed by lowered sea level, although
196 these are considered in the full LGM experiment. The full LGM and MH experiments include



197 changes to both air pressure and tree cover; these are not considered in the factorial experiments
 198 because preliminary analyses indicated that the impact of these changes on simulated global
 199 GPP was less than 0.2PgC and therefore negligible.

200
 201 **3. Results**

202 Simulated global GPP at the LGM was 83.9 PgC (Table 1), considerably lower than the
 203 simulated global value during the pre-industrial period (109.6 PgC). The largest reductions in
 204 GPP compared to the pre-industrial baseline were in the northern hemisphere extra-tropics
 205 (Figure 2, Table 2), which experienced a more than 50% reduction in GPP. There was a more
 206 modest decrease (13%) in the southern extra-tropics and only a small decrease in the tropics
 207 (3%). Part of the reduction (10.5 PgC) in global GPP reflects the loss of vegetation from areas
 208 that were covered by ice at the LGM; this was only partially compensated by vegetation growth
 209 on the continental shelves exposed by the reduced sea level (8.3 PgC). Although there was a
 210 reduction overall and across most of the world, some regions experienced a small increase in
 211 productivity at the LGM compared to the PI (Figure 3). These are all in now-arid regions and
 212 the increase therefore presumably reflects the fact that moisture constraints on vegetation
 213 growth were reduced in the colder climate of the LGM.

214
 215 **Table 1:** Contribution to global changes in gross primary production (GPP) in the Last Glacial
 216 Maximum (LGM), the mid-Holocene (MH), and the pre-industrial (PI) experiments. The table
 217 gives the global total in each experiment, the GPP of land exposed by lowered sea level at the
 218 LGM, the GPP of land that was covered by ice sheets at the LGM and was exposed in the MH
 219 and PI experiments, and GPP for the land area in common between all three experiments.

	Total non-glaciated land area	Land area covered by ice at LGM	Land area exposed by lowered sea level at LGM	Common land area between the experiments
GPP LGM	83.9 PgC	n/a	8.3 PgC	75.5 PgC
GPP MH	110.3 PgC	10.6 PgC	n/a	99.6 PgC
GPP PI	109.6 PgC	10.5 PgC	n/a	99.1 PgC

221

222

223 **Table 2:** Regional contributions to total annual gross primary production (GPP) in the tropics,
 224 the northern extra-tropics (NET) and the southern extra-tropics (SET) in the Last Glacial
 225 Maximum (LGM), the mid-Holocene (MH), and the pre-industrial (PI) experiments.

226

	LGM	MH	PI
Tropics (25°N-25S)	56.4 PgC	57.7 PgC	58.3 PgC
NET (>25°N)	21.4 PgC	46.2 PgC	44.3 PgC
SET (>25°S)	6.0 Pg C	6.4 PgC	6.9 PgC

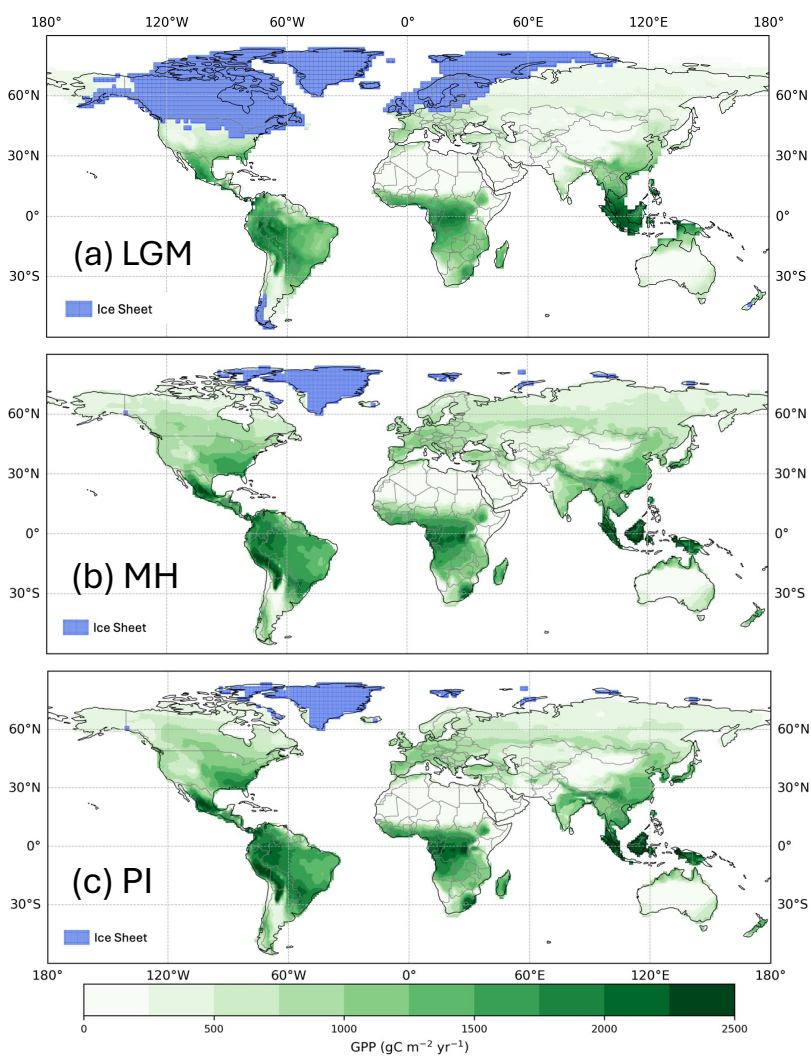
227

228

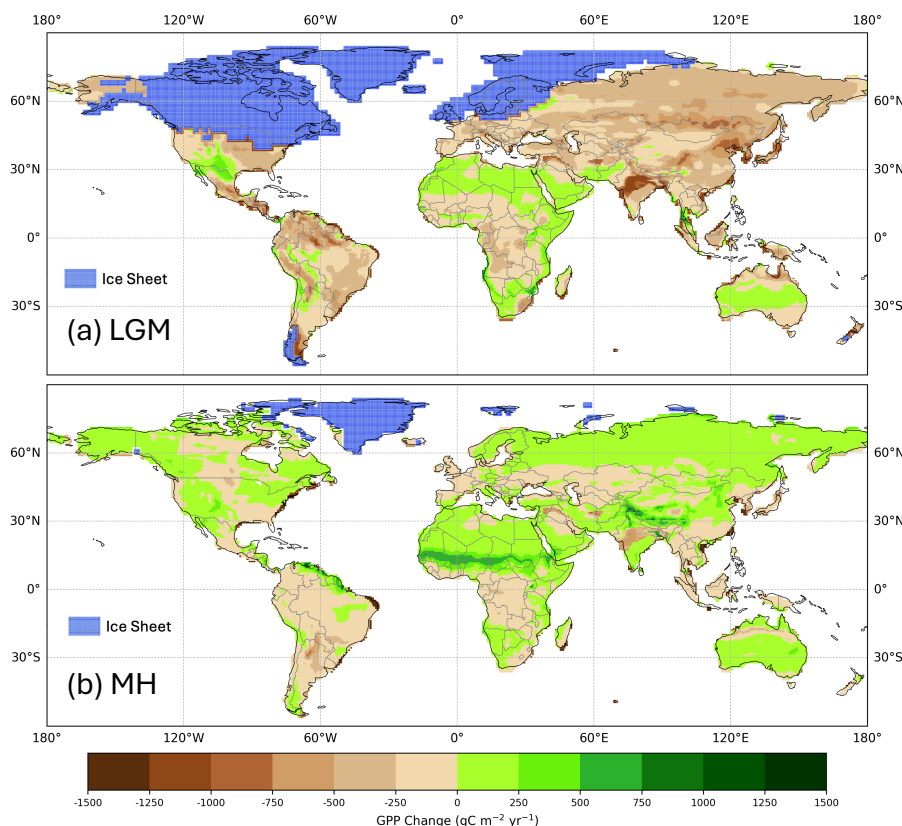
229 Simulated GPP increased to 110.3 PgC in the MH compared to 83.9 PgC at the LGM. Part of
 230 this increase (10.6 PgC) was a result of vegetation growth in areas that were covered by ice
 231 sheets during the LGM. However, there were notable increases in the non-glaciated high
 232 latitudes (northern Siberia and Beringia), in tropical regions, and in areas influenced by MH
 233 monsoon expansion (Sahel, south-east Asia, southern African savannas and the South
 234 American cerrado) (Figure 2). GPP increased in the common area between the LGM and MH



235 experiments by ca 32% (Table 1), with the largest increase in the NET (Table 2). The transition
236 from the MH to the PI resulted in a very small decrease in global GPP (Figure 3. Simulated
237 GPP in the MH was slightly higher (4%) than in the PI experiment in the northern extra-tropics,
238 although still lower than in the PI in other regions (Table 2).
239



240
241 **Figure 2:** Simulated total annual gross primary production (GPP). The plots show simulated
242 GPP for (a) the Last Glacial Maximum (LGM), (b) the mid-Holocene (MH), and (c) the pre-
243 industrial (PI).
244



245

246 **Figure 3:** Simulated change in total annual gross primary production (GPP) between the pre-
 247 industrial (PI) and (a) the Last Glacial Maximum (LGM) and (b) the mid-Holocene (MH).

248

249

250

251

252

253

254

255

256

257

258

259

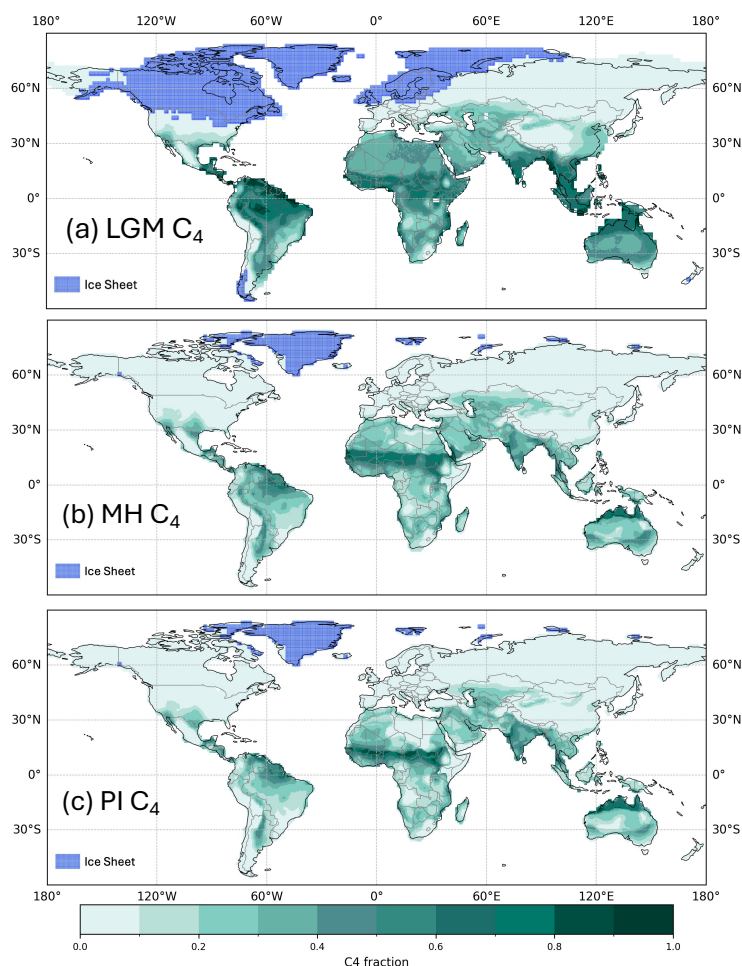
These changes in GPP were accompanied by a shift in the relative importance of C₃ and C₄ plants (Table 3, Figure 4). C₄ plants represented 23% and 25% of the vegetation fraction in the PI and MH experiments respectively, but 40% of the vegetation fraction at the LGM. C₄ plants were responsible for 56% of the total GPP at the LGM compared to 25% and 21% in the MH and PI respectively. The fraction of C₄ plants increased across most regions of the world at the LGM (Supplementary Figure 1), but in some regions including the Central Great Plains of North America, the northern Sahel, and the Tibetan Plateau and part of the Loess Plateau in northeastern China C₄ plants were less abundant than in the PI. The areas where C₄ plants were less abundant in the MH than in the PI were more extensive (Supplementary Figure 1) and are primarily in regions of northern Africa and Asia influenced by the expansion of the monsoons.

Table 3: Changes in C₃/C₄ fraction and contribution of C₃/C₄ vegetation to total GPP

	LGM	MH	PI
Global average C ₄ fraction	40%	25%	23%
Global average C ₃ contribution of total annual GPP (gC m ² yr)	281.4	608.9	618.6
Global C ₃ contribution to total GPP (PgC)	37.1	82.8	86.2
Global average C ₄ contribution of total annual GPP (gC m ² yr)	297.7	166.3	140.5
Global C ₄ contribution to total GPP (PgC)	46.8	27.5	23.4



260



261

262

263

Figure 4. Global C_4 fraction distribution for (a) the Last Glacial Maximum (LGM), (b) the mid-Holocene (MH), and (c) the pre-industrial (PI).

264

265

266

267

268

269

270

271

272

The factorial experiments showed that the changes in climate and CO_2 had a large negative effect on GPP at the LGM, while light (PPFD) had a small positive effect (Table 4, Figure 5). The shift to a colder, drier climate had a somewhat larger negative effect on plant productivity (-14.8 PgC) than the reduction in CO_2 (-12.2 PgC). Climate has a major impact on reducing GPP in the high- to mid-latitudes of North America and Eurasia (Figure 6a, Supplementary Figure 2) but changes due to the lowering of CO_2 were almost as important (Figure 6b, Supplementary Figure 3). Changes in climate (Supplementary Figure 2), most likely the overall reduction in precipitation (Supplementary Figure 5), was the most important factor causing reduced GPP in northern Amazonia, India and north-western China. However, the cooler



273 climate had a positive effect on GPP in regions that are semi-arid today (Supplementary Figure
274 2, Supplementary Figure 5). Changes in PPFD were the dominant factor in increasing GPP at
275 the margin at the northernmost edge of the vegetated zone downwind of the Scandinavian ice
276 sheet and into Beringia (Supplementary Figure 4).

277 The two-way synergy between climate and CO₂ was positive (Table 4, Figure 5), i.e. the change
278 in GPP is less than would be expected if the impacts were additive. This reflects the fact that,
279 whereas lower temperatures favour C₃ plants, lower CO₂ offsets this and promotes the
280 expansion of C₄ plants over much of the globe (Supplementary Figures 6, 7). C₄ plants were
281 especially favoured in tropical regions, where the climate changes were relatively muted, and
282 the changes in CO₂ correspondingly more influential. The synergies of both climate and CO₂
283 with PPFD, although small (0.9 and 0.2 PgC respectively) are negative. The synergy between
284 climate and PPFD probably reflects the fact reduced cloud cover in drier climates
285 (Supplementary Figure 6, 8). The synergy between CO₂ and PPFD stems from the fact that
286 both low CO₂ and high PPFD favour C₄ plants, increasing GPP particularly in the extratropics
287 (Supplementary Figure 7, 8).

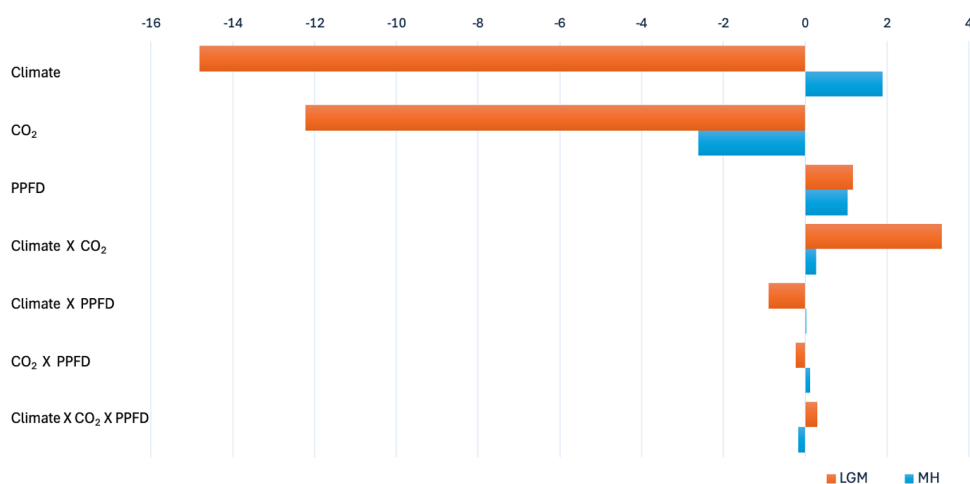
288 Climate changes had a positive effect on GPP in the mid-Holocene (Table 4, Figure 5). This
289 likely reflects the impact of increased precipitation in now semi-arid regions due to monsoon
290 expansion combined with warmer growing seasons in the high northern latitudes, both
291 consequences of the orbitally-induced changes in solar radiation (Supplementary Figure 5).
292 These experiments also show that changes in PPFD have a positive effect on plant growth,
293 particularly in the northern mid- to high latitudes and in now-arid regions (Supplementary
294 Figure 4). The positive impact in northern mid- to high latitudes appears to be due to
295 enhancement of growing season conditions for C₃ plants, while the positive impact in now-arid
296 regions reflects an increase in C₄ plants (Supplementary Figure 8). However, the reduction of
297 CO₂ compared to the PI state (16 ppm) resulted in a much larger overall reduction in GPP than
298 the enhancements due to climate or PPFD changes (Supplementary Figure 3). The impact of
299 the lower CO₂ in the mid-Holocene is the dominant factor causing reductions in GPP in
300 southern China, the southern hemisphere tropical and savanna regions in Africa, and in the
301 cerrado of South America (Figure 6). The two-way synergies between the three drivers are all
302 positive, but small (Table 4, Figure 5).



303 **Table 4.** Stein-Alpert decomposition of the impact of changes in climate, CO₂ and light
 304 (photosynthetic photon flux density, PPFD), and their synergies, on gross primary production
 305 (GPP) at the Last Glacial Maximum (LGM) and in the mid-Holocene (MH) compared to the
 306 pre-industrial (PI) simulations. Note that the baseline GPP value for the LGM is for the
 307 common land area between this experiment and the PI simulation and is therefore smaller than
 308 the baseline GPP value for the MH decomposition.
 309

Experiment	Stein-Alpert decomposition	Climate	CO ₂	PPFD	GPP (PgC)
LGM	f0	PI	PI	PI	99.1
	f1, LGM	LGM	PI	PI	84.3
	f2, LGM	PI	LGM	PI	86.9
	f3, LGM	PI	PI	LGM	100.3
	f12, LGM	LGM	LGM	PI	75.4
	f13, LGM	LGM	PI	LGM	84.6
	f23, LGM	PI	LGM	LGM	87.8
	f123, LGM	LGM	LGM	LGM	75.7
MH	f0	PI	PI	PI	109.6
	f1, MH	MH	PI	PI	111.5
	f2, MH	PI	MH	PI	107.0
	f3, MH	PI	PI	MH	110.6
	f12, MH	MH	MH	PI	109.1
	f13, MH	MH	PI	MH	112.5
	f23, MH	PI	MH	MH	108.1
	f123, MH	MH	MH	MH	110.1

310
 311
 312

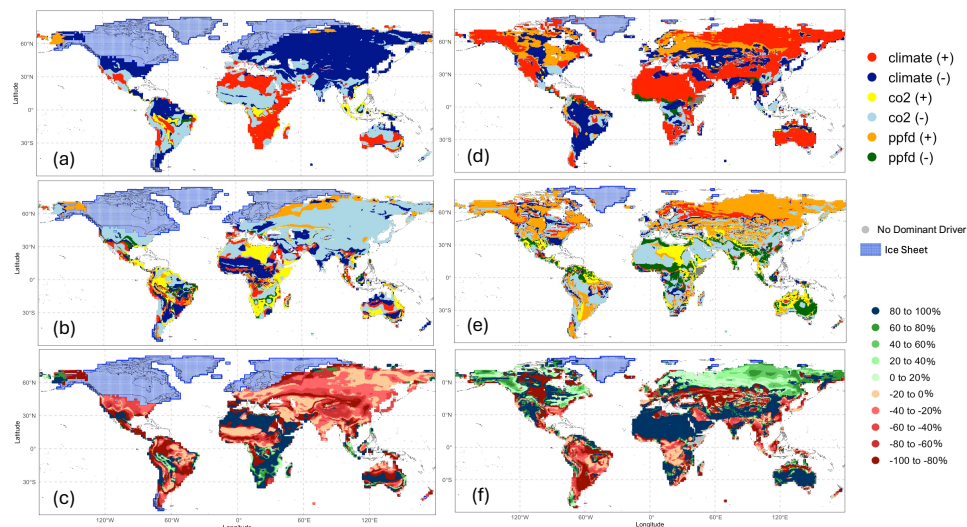


313
 314
 315
 316
 317
 318

314 **Figure 5.** Impact of climate, light and CO₂ on the changes in gross primary production (GPP,
 315 PgC) at the Last Glacial Maximum (LGM) and the mid-Holocene (MH) compared to the
 316 pre-industrial (PI) period. Note that the results are based on the common land area between each
 317 experiment and the PI simulation.



319



320

321 *Figure 6. Global distribution of (a) main drivers and constraints (b) secondary drivers and*
 322 *constraints and (c) the proportional difference (percentage) of total change between the main*
 323 *and the secondary driver on gross primary production (GPP) at the Last Glacial Maximum*
 324 *(LGM) compared to the pre-industrial (PI) experiment; and (d) main drivers and constraints*
 325 *(e) secondary drivers and constraints (f) the proportional difference (percentage) of total*
 326 *change between the main and the secondary driver on gross primary production (GPP) in the*
 327 *Mid-Holocene (MH) compared to the pre-industrial (PI) experiment.*

328

329 **4. Discussion**

330

331 We have shown that the LGM was characterised by a large reduction in modelled GPP, while
 332 the mid-Holocene was characterised by a small increase in GPP compared to the pre-industrial
 333 state. The simulated reduction at the LGM is consistent with previous model-based estimates
 334 (e.g. Francois et al., 1998; Prentice et al., 2011; Hoogakker et al., 2016), including those from
 335 the latest phase of the Couple Model Intercomparison project (CMIP6/PMIP4: Supplementary
 336 Table 3). However, there is a considerable range in the magnitude of these modelled estimates,
 337 reflecting differences in both the simulated LGM climate and in the vegetation model used.
 338 Our estimate of the GPP at the LGM (84 PgC) is in the middle of the range of the
 339 CMIP6/PMIP4 models (61-109 PgC). There have been a limited number of studies that have
 340 estimated GPP at the LGM by constraining model estimates using oxygen isotope records from
 341 ice core (Landais et al., 2007; Ciais et al., 2011; Yang et al., 2022). These show a similarly
 342 large range in simulated GPP (40-110 PgC), in part because of the uncertainties associated with
 343 estimating ocean productivity and respiration fractionation rates. Thus, although there is a
 344 consensus that GPP was considerably lower at the LGM than during pre-industrial times, and
 345 this is consistent with pollen evidence for a very large reduction in tree cover over much of the
 346 world (Prentice et al., 2000; Williams, 2003; Pickett et al., 2004; Marchant et al., 2009), the
 absolute magnitude of this change is uncertain.

347

348 The modelled abundance of C₄ plants was nearly double at the LGM compared to the pre-
 349 industrial era (40% versus 23% of the vegetation fraction) and that C₄ vegetation was
 responsible for 56% of the total modelled GPP at that time. These changes are broadly



350 consistent with pollen-based reconstructions, indicating a substantial reduction in tree cover at
351 the LGM (Prentice et al., 2000). However, while pollen data can be used discriminate between
352 trees (virtually all C₃) and grasses, it cannot be used to infer changes in the importance of C₃
353 and C₄ grasses. Compound-specific δ¹³C analyses of leaf wax biomarkers provide evidence of
354 the relative contribution of C₃ and C₄ plants (Eglinton & Eglinton, 2008; Diefendorf et al.,
355 2010) and have shown that C₄ plants were more abundant at the LGM than during the Holocene
356 in many regions of the world (e.g. in southern Africa: Rommerskirchen et al., 2006; Vogts et
357 al., 2012; eastern Africa: Sinninghe Damsté et al., 2011; Himalayan Basin: Galy et al., 2008;
358 southern China: Jiang et al., 2019; south-western North America: Cotton et al., 2016; northern
359 South America: Makou et al., 2007), consistent with our simulations. There are a few regions
360 where C₄ plants were less abundant at the LGM than during the Holocene, including the
361 Chinese Loess Plateau and the Great Plains of North America (Cotton et al., 2016). Both of
362 these regions are identified as characterised by reduced C₄ abundance in our simulations. A
363 number of modelling studies have shown that C₄ plants were globally more abundant at the
364 LGM (e.g. Harrison & Prentice, 2003; Bragg et al., 2013; Martin Calvo & Prentice, 2015) but
365 did not quantify the relative contribution of C₄ plants to global GPP. Thus, our analyses are
366 consistent with previous studies of the nature of the shift in vegetation composition at the LGM
367 and provide, for the first time, a quantitative estimate of the magnitude of this change.

368 Climate has a negative effect on GPP at the LGM but a positive effect in the MH. The LGM
369 climate was globally colder and drier, although the largest changes in both temperature and
370 precipitation were in the northern mid- to high-latitudes (Kageyama et al., 2021). This is
371 reflected in our simulations; the overall reduction in GPP compared to the pre-industrial
372 baseline in the northern extra-tropics was 52%, far larger than the reductions in the southern
373 extra-tropics (13%) or the tropics (3%). The cooling in the ice-free regions of the northern
374 extra-tropics reflects advection of cold air temperatures downwind from the ice sheets, while
375 the drying largely reflects the temperature-induced reduction in evaporation and precipitation
376 recycling (Izumi et al., 2013; Li et al., 2013; Kageyama et al., 2021). The positive effect of
377 climate on GPP in the MH reflects changes in precipitation in now semi-arid regions of the
378 sub-tropics as a result of the expansion of the northern hemisphere monsoons and a lengthening
379 of the growing season in the northern mid- to high-latitudes as a result of increased solar
380 radiation in summer (Brierley et al., 2020). These changes in climate are reflected in our
381 simulations; although the northern extra-tropics are the only region to show an overall increase
382 in GPP compared to the pre-industrial (4%), regions influenced by monsoon expansion, such
383 as the Sahel and parts of Asia, also show increased GPP.

384 The impact of lowered CO₂ on GPP is only slightly smaller than the changes caused by climate
385 at the LGM, reinforcing the overall reduction of GPP at the LGM. The impact of lowered CO₂
386 on GPP in the MH is larger than the impact of climate, offsetting the positive impacts of climate
387 change in the MH experiment. The importance of CO₂ in driving vegetation changes has been
388 widely commented on for the LGM (Poley et al., 1993; Jolly & Haxeltine, 1997; Cowling &
389 Sykes, 1999; Harrison & Prentice, 2003; Flores et al., 2009; Prentice et al., 2011; Bragg et al.,
390 2013; Martin Calvo & Prentice, 2015) and in the context of ongoing and future climate changes
391 (Piao et al., 2006; Keenan et al., 2014; Archer et al., 2017; Haverd et al., 2020; Piao et al.,
392 2020) but its role in offsetting the positive impacts of climate change in the MH has not been
393 widely noted. Despite the comparatively small change in CO₂ between the PI and MH (20
394 ppm), according to our simulations the lowering of CO₂ would have reduced GPP by ca 3 PgC
395 whereas the increase produced by the change in climate is only 2 PgC.



396 We have derived climate inputs from the MPI ESM. When compared to reconstructions of both
397 marine and terrestrial climate variables, the MPI ESM has been shown to be among the best-
398 performing models both for the LGM and the mid-Holocene (Brierley et al., 2020; Kageyama
399 et al., 2021). Nevertheless, the use of a single climate model is a limitation of this study. It
400 would be useful to repeat these analyses with a wider range of models that have made
401 palaeoclimate simulations of these two key periods, but the constraint is that most of these
402 models do not provide information on changes in tree cover that is to run the C₃/C₄ competition
403 model.

404

405 **5. Conclusions**

406 Eco-evolutionary optimality approaches provide a robust way of modelling vegetation changes
407 under different climate regimes. We compared simulated changes in GPP and C₃/C₄ plant
408 abundance in a cold glacial and a warm interglacial period relative to the pre-industrial state.
409 We showed that the colder, drier climate at the LGM substantially decreases GPP and the
410 warmer, wetter climate of the MH increases GPP. Changes in vegetation productivity caused
411 by the lower CO₂ in both intervals compared to the pre-industrial contributed to the reduction
412 of GPP at the LGM and was sufficient to annul the positive impacts of climate on GPP during
413 the MH. These results point to the importance of a realistic treatment of the direct physiological
414 impacts of CO₂ on plant growth to simulate realistic ecosystem changes, both in the past and
415 in the future.

416 **Data Availability**

417 The CMIP6 MPI-ESM1-2-LR outputs are accessible via the Earth System Grid Federation
418 (ESGF) at <http://esgf-node.llnl.gov/search/cmip6/> (last accessed: 2 December 2024).
419 Interpolated input data and derived outputs related to this study are available at DOI:
420 10.5281/zenodo.14257604. The documentation for the P model, the C₃/C₄ competition model,
421 and the SPLASH model can be found at [DOI: 10.5281/zenodo.8366848](https://doi.org/10.5281/zenodo.8366848) (Orme and Marion,
422 2023). The codes used for model coupling and experiment analysis used in this paper is
423 available at DOI: 10.5281/zenodo.14257604.

424 **Supplement.**

425 Supplementary Information is available for this paper.

426 **Author Contributions**

427 JZ, SPH and ICP designed the study. BZ provided model code. JZ ran the experiments. JZ and
428 SPH conducted the analyses. SPH wrote the first version of the manuscript and all co-authors
429 contributed to the final version.

430 **Competing Interests**

431 None of the authors has any competing interests.

432 **Financial Support and Acknowledgements**

433 JZ and SPH acknowledge NERC funding for the project "When and Why does it Rain in the
434 Desert: Utilising unique stalagmite and dust records on the northern edge of the Sahara". This
435 work is a contribution to the LEMONTREE (Land Ecosystem Models based On New Theory,
436 obseRvations and ExperimEnts) project (SPH, ICP). LEMONTREE research received support
437 through Schmidt Sciences. ICP also acknowledges funding from the European Research
438 Council for the project REALM (Re-inventing Ecosystem And Land-surface Models, Grant
439 Number 787203).

440



441 **References**

- 442 Archer, S.R., Andersen, E.M., Predick, K.I., Schwinning, S., Steidl, R.J., and Woods, S.R.:
443 Woody plant encroachment: Causes and consequences. In: Briske, D. (Ed.),
444 Rangeland Systems. Springer Series on Environmental Management. Springer, Cham.
445 https://doi.org/10.1007/978-3-319-46709-2_2, 2017.
- 446 Berger, A. L.: Long-term variations of caloric insolation resulting from the earth's orbital
447 elements, *Quat. Res.*, 9, 139–167, 1978.
- 448 Berger, A., and Loutre, M. F.: insolation values for the climate of the last 10 000 000 years,
449 *Quat. Sci. Rev.*, 10, 297–317, [https://doi.org/10.1016/0277-3791\(91\)90033-q](https://doi.org/10.1016/0277-3791(91)90033-q), 1991.
- 450 Bonan, G. B.: Forests and climate change: Forcings, feedbacks, and the climate benefits of
451 forests, *Science*, 320, 1444–1449, 2008.
- 452 Bragg, F., Prentice, I.C., Harrison, S.P., Foster, P.N., Eglinton, G., Rommerskirchen F., and
453 Rullkötter, J.: n-Alkane stable isotope evidence for CO₂ as a driver of vegetation
454 change, *Biogeosci.*, 10, 2001–2010, 2013.
- 455 Brierley, C., Zhao, A., Harrison, S.P., Braconnot, P., Williams, C., Thornalley, D., Shi, X.,
456 Peterschmitt, J-Y., Ohgaito, R., Kaufman, D.S., Kagayama, M., Hargreaves, J.C., Erb,
457 M., Emile-Geay, J., D'Agostino, R., Chandan, D., Carré, M., Bartlein, P.J., Zheng, W.,
458 Zhang, Z., Zhang, Q., Yang, H., Volodin, E.M., Routsen, C., Peltier, W.R., Otto-
459 Bliessner, B., Morozova, P.A., McKay, N.P., Lohmann, G., LeGrande, A.N., Guo, C.,
460 Cao, J., Brady, E., Annan, J.D., and Abe-Ouchi, A.: Large-scale features and evaluation
461 of the PMIP4-CMIP6 *midHolocene* simulations, *Clim. Past*, 16, 1847-1872, 2020.
- 462 Cai, W., and Prentice, I.C.: Recent trends in gross primary production and their drivers:
463 analysis and modelling at flux-site and global scales, *Environ. Res. Lett.*, 15, 124050,
464 2020.
- 465 Cai, W., Zhu, Z., Harrison, S.P., Ryu, Y., Wang, H., Zhou, B., and Prentice, I.C.: A unifying
466 principle for global greenness patterns and trends. *BioRxiv*
467 doi: <https://doi.org/10.1101/2023.02.25.529932> (2023) *Nat. Comm. Environ.*, in
468 review, 2024.
- 469 Chen, J.M., Ju, W., Ciais, P., Viovy, N., Liu, R., Liu, Y., and Lu, X.: Vegetation structural
470 change since 1981 significantly enhanced the terrestrial carbon sink, *Nat.*
471 *Commun.*, 10, 4259, <https://doi.org/10.1038/s41467-019-12257-8>, 2019.
- 472 Ciais, P., Tagliabue, A., Cuntz, M., Bopp, L., Scholze, M., Hoffmann, G., Lourantou, A.,
473 Harrison, S.P., Prentice, I.C., Kelley, D.I., Kovan, C. and Piao, S.L.: Large inert
474 carbon pool in the terrestrial biosphere at the Last Glacial Maximum, *Nature Geosci.*,
475 5, 74-79, 10.1038/NCEO1324, 2011.
- 476 Cotton, J.M., Cerling, T.E., Hoppe, K.A., Mosier, T.M., and Still, C.J.: Climate, CO₂, and the
477 history of North American grasses since the Last Glacial Maximum, *Sci. Adv.*, 2,
478 e1501346, doi:10.1126/sciadv.1501346, 2016.
- 479 Cowling, S.A., and Sykes, M.T.: Physiological significance of low atmospheric CO₂ for
480 plant-climate interactions. *Quat. Res.* 52, 237–242, 1999.
- 481 Davis, T.W., Prentice, I.C., Stocker, B.D., Thomas, R.T., Whitley, R.J., Wang, H., Evans, B.
482 J., Gallego-Sala, A.V., Sykes, M.T., and Cramer, W.: Simple process-led algorithms
483 for simulating habitats (SPLASH v.1.0): robust indices of radiation,
484 evapotranspiration and plant-available moisture, *Geosci. Model Dev.*, 10, 689–708,
485 <https://doi.org/10.5194/gmd-10-689-2017>, 2017.
- 486 Diefendorf, A. F., Mueller, K. E., Wing, S. L., Koch, P. L., and Freeman, K. H.: Global
487 patterns in leaf ¹³C discrimination and implications for studies of past and future
488 climate, *P. Natl. Acad. Sci. USA*, 107, 5738–5743, 2010.
- 489 Eglinton, T. I. and Eglinton, G.: Molecular proxies for paleoclimatology. *Earth Planet. Sci.*
490 *Lett.*, 275, 1–16, 2008.



- 491 Farquhar, G.D., von Caemmerer, S., and Berry, J.A.: A biochemical model of photosynthetic
492 CO₂ assimilation in leaves of C₃ species, *Planta*, 149, 78–90, 1980.
- 493 Flores, O., Gritti, E.S., and Jolly, D.: Climate and CO₂ modulate the C₃/C₄ balance and δ¹³C
494 signal in simulated vegetation, *Clim. Past*, 5, 431–440, 2009.
- 495 Forzieri, G., Miralles, D. G., Ciais, P., Alkama, R., Ryu, Y., Duveiller, G., Zhang, K.,
496 Robertson, E., Kautz, M., Martens, B., Jiang, C., Arno, A., Georgievski, G., Li, W.,
497 Ceccherini, G., Anthoni, P., Lawrence, P., Wiltshire, A., Pongratz, J., ... Cescatti, A.:
498 Increased control of vegetation on global terrestrial energy fluxes, *Nature Clim.*
499 *Change*, 10, 356–362. <https://doi.org/10.1038/s41558-020-0717-0>, 2020.
- 500 François, L.M., Delire, C., Warnant, P., and Munhoven, G.: Modelling the glacial–interglacial
501 changes in the continental biosphere, *Glob. Planet. Change*, 16–17, 37–52,
502 [https://doi.org/10.1016/S0921-8181\(98\)00005-8](https://doi.org/10.1016/S0921-8181(98)00005-8), 1998.
- 503 Galy, V., François, L., France-Lanord, C., Faure, P., Kudrass, H., Palhol, F., and Singh, S.K.:
504 C₄ plants decline in the Himalayan basin since the Last Glacial Maximum, *Quat. Sci.*
505 *Rev.*, 27, 1396–1409, <https://doi.org/10.1016/j.quascirev.2008.04.005>, 2008.
- 506 Gerhart, L.M., and Ward, J.K.: Plant responses to low [CO₂] of the past, *New Phytol.*, 188:
507 674–695, <https://doi.org/10.1111/j.1469-8137.2010.03441.x>, 2010.
- 508 Harrison, S.P., and Prentice, I.C.: Climate and CO₂ controls on global vegetation distribution
509 at the last Glacial Maximum: analysis based on palaeovegetation data, biome
510 modelling and palaeoclimate simulations, *Glob. Chang. Biol.*, 9, 983–1004, 2003
- 511 Haverd, V., Smith, B., Canadell, J.G., Cuntz, M., Mikaloff-Fletcher, S., Farquhar, G.,
512 Woodgate, W., Briggs, P.R., and Trudinger, C.M.: Higher than expected CO₂
513 fertilization inferred from leaf to global observations, *Glob. Chang. Biol.* 26, 2390–
514 2402, <https://doi.org/10.1111/gcb.14950>, 2020.
- 515 Hoek van Dijke, A. J., Mallick, K., Schlerf, M., Machwitz, M., Herold, M., and Teuling, A.
516 J.: Examining the link between vegetation leaf area and land–atmosphere exchange of
517 water, energy, and carbon fluxes using FLUXNET data, *Biogeosci.*, 17, 4443–4457,
518 <https://doi.org/10.5194/bg-17-4443-2020>, 2020.
- 519 Hoogakker, B.A.A., Smith, R.S., Singarayer, J.S., Marchant, R., Prentice, I.C., Allen, J.R.M.,
520 Anderson, R.S., Bhagwat, S.A., Behling, H., Borisova, O., Bush, M., Correa-Metrio,
521 A., de Vernal, A., Finch, J.M., Fréchet, B., Lozano-Garcia, S., Gosling, W.D.,
522 Granoszewski, W., Grimm, E.C., Grüger, E., Hanselman, J., Harrison, S.P., Hill, T.R.,
523 Huntley, B., Jiménez-Moreno, G., Kershaw, P., Ledru, M-P., Magri, D., McKenzie, M.,
524 Müller, U., Nakagawa, T., Novenko, E., Penny, D., Sadori, L., Scott, L., Stevenson, J.,
525 Valdes, P.J., Vandergoes, M., Velichko, A., Whitlock, C., and Tzedakis, C.: Terrestrial
526 biosphere changes over the last 120 kyr, *Clim. Past*, 12, 51–73,
527 <https://doi.org/10.5194/cp-12-51-2016>, 2016.
- 528 Izumi, K., Bartlein, P.J., and Harrison, S.P.: Consistent behaviour of the climate system in
529 response to past and future forcing, *Geophys. Res. Lett.*, 40, 1817–1823,
530 [doi:10.1002/grl.50350](https://doi.org/10.1002/grl.50350), 2013.
- 531 Jiang, C., Ryu, Y., Wang, H., and Keenan, T.F.: An optimality-based model explains seasonal
532 variation in C₃ plant photosynthetic capacity, *Glob. Change Biol.*, 26, 6493–6510,
533 2020.
- 534 Jiang, W., Wu, H., Li, Q., Lin, Y., and Yu, Y.: Spatiotemporal changes in C₄ plant abundance
535 in China since the Last Glacial Maximum and their driving factors, *Palaeogeog.,*
536 *Palaeoclim., Palaeoecol.*, 518, 10–21, <https://doi.org/10.1016/j.palaeo.2018.12.021>,
537 2019.
- 538 Jolly, D., and Haxeltine, A.: Effect of low glacial atmospheric CO₂ on tropical African
539 montane vegetation, *Science*, 276, 786–788, 1997.



- 540 Kaplan, J.O., Bigelow, N.H., Bartlein, P.J., Christensen, T.R., Cramer, W., Harrison, S.P.,
541 Matveyeva, N.V., McGuire, A.D., Murray, D.F., Prentice, I.C., Razzhivin, V.Y., Smith,
542 B. and Walker, D.A., Anderson, P.M., Andreev, A.A., Brubaker, L.B., Edwards, M.E.,
543 and Lozhkin, A.V.: Climate change and Arctic ecosystems II: Modeling, palaeodata-
544 model comparisons, and future projections, *J. Geophys. Res.- Atmos.*, 108, 8171. doi:
545 10.1029/2002JD002559, 2003.
- 546 Kageyama, M., Albani, S., Braconnot, P., Harrison, S.P., Hopcroft, P.O., Ivanovic, R.F.,
547 Lambert, F., Marti, O., Peltier, W.R., Peterschmidt, J.-Y., Roche, D.M., Tarasov, L.,
548 Zhang, X., Brady, E., Haywood, A.M., LeGrande, A., Lunt, D.J., Mahowald, N.M.,
549 Mikolajewicz, U., Nisancioglu, K.H., Otto-Bliesner, B.L., Renssen, H., Tomas, B.,
550 Zhang, Q., Abe-Ouchi, A., Bartlein, P.J., Cao, J., Lohmann, G., Ohgaito, R., Shi, X.,
551 Volodin, E., Yoshida, K., Zhang, X., and Zheng, W.: The PMIP4 contribution to CMIP6
552 – Part 4: Scientific objectives and experimental design of the PMIP4-CMIP6 Last
553 Glacial Maximum experiments and PMIP4 sensitivity experiments, *Geosci. Model*
554 *Dev.*, 10, 4035-4055, <https://doi.org/10.5194/gmd-10-4035-2017>, 2017
- 555 Kageyama, M., Harrison, S.P., Kapsch, M., Lofverstrom, M., Lora, J.M., Mikolajewicz, U.,
556 Sherriff-Tadano, S., Vadsaria, T., Abe-Ouchi, A., Bouttes, N., Chandan, D., LeGrande,
557 A.N., Lhardy, F., Lohmann, G., Morozova, P.A., Ohgaito, R., Peltier, W.R., Quiquet,
558 A., Roche, D.M., Shi, X., Schmittner, A., Tierney, J.E., and Volodin, E.: The PMIP4-
559 CMIP6 Last Glacial Maximum experiments: preliminary results and comparison with
560 the PMIP3-CMIP5 simulations, *Clim. Past*, 17, 1065-1089, 2021.
- 561 Keenan, T.F., Hollinger, D.Y., Bohrer, G., Dragoni, D., Munger, J.W., Schmid, H.P., and
562 Richardson, A.D.: Increase in forest water-use efficiency as atmospheric carbon
563 dioxide concentrations rise, *Nature*, 499, 324–327, 2013.
- 564 Landais, A., Lathiere, J., Barkan, E., and Luz, B.: Reconsidering the change in global
565 biosphere productivity between the Last Glacial Maximum and present day from the
566 triple oxygen isotopic composition of air trapped in ice cores, *Glob. Biogeochem.*
567 *Cyc.*, 21, GB1025, 2007.
- 568 Lavergne, A., Harrison, S.P., Atsawawaranunt, K., Dong, N., and Prentice, I.C.: Recent C₄
569 vegetation decline is imprinted in land carbon isotopes. *Nature Comm. Earth Environ.*,
570 in review, 2024
- 571 Li, G., Harrison, S. P., Bartlein, P. J., Izumi, K., and Prentice, I. C.: Precipitation scaling with
572 temperature in warm and cold climates: an analysis of CMIP5 simulations, *Geophys.*
573 *Res. Lett.*, 40, 4018– 4024, <https://doi.org/10.1002/grl.50730>, 2013.
- 574 Makou, M.C., Hughen, K.A., Xu, L., Sylva, S.P., and Eglinton, T.I.: Isotopic records of tropical
575 vegetation and climate change from terrestrial vascular plant biomarkers preserved in
576 Cariaco Basin sediments, *Org. Geochem.*, 38, 1680-1691,
577 <https://doi.org/10.1016/j.orggeochem.2007.06.003>, 2007.
- 578 Marchant, R.A., Harrison, S.P., Hooghiemstra, H., Markgraf, V., Boxel, J.H., Ager, T., Almeida,
579 L., Anderson, R., Baied, C., Behling, H., Berrío, J.C., Burbidge, R., Björck, S., Byrne,
580 R., Bush, M.B., Cleef, A.M., Duivenvoorden, J.F., Flenley, J.R., de Oliveira, P.E., van
581 Geel, B., Graf, K.J., Gosling, W.D., Harbele, S., van der Hammen, T., Hansen, B.C.S.,
582 Horn, S.P., Islebe, G.A., Kuhry, P., Ledru, M-P., Mayle, F.E., Leyden, B.W., Lozano-
583 Garcia, M.S., Lozano-Garcia, S., Melief, A.B.M., Moreno, P., Moar, N.T., Prieto, A.,
584 van Reenan, G.B., Salgado-Labouriau, M.L., Schäbitz, F., Schreve-Brinkman, E.J., and
585 Wille, M.: Pollen-based biome reconstructions for Latin America at 0, 6000 and 18 000
586 radiocarbon years, *Clim. Past*, 5, 725-767, 2009
- 587 Martin Calvo, M., and Prentice, I.C.: Effects of fire and CO₂ on biogeography and primary
588 production in glacial and modern climates, *New Phytol.*, 208, 987-994, 2015.



- 589 Mauritsen, T., Bader, J., Becker, T., Behrens, J., Bittner, M., Brokopf, R., et al.:
590 Developments in the MPI-M Earth System Model version 1.2 (MPI-ESM1.2) and its
591 response to increasing CO₂, *J. Advan. Modeling Earth Systems*, 11, 998–
592 1038, <https://doi.org/10.1029/2018MS001400>, 2019.
- 593 Medlyn, B.E., De Kauwe, M.G., Lin, Y.-S., Knauer, J., Duursma, R.A., Williams, C.A., Arneth,
594 A., Clement, R., Isaac, P., Limousin, J.-M., Linderson, M.-L., Meir, P., Martin-StPaul,
595 N., and Wingate, L.: How do leaf and ecosystem measures of water-use efficiency
596 compare?, *New Phytol.*, 216, 758–770, <https://doi.org/10.1111/nph.14626>, 2017.
- 597 Otto-Bliesner, B.L., Braconnot, P., Harrison, S.P., Lunt, D.J., Abe-Ouchi, A., Albani, S.,
598 Bartlein, P.J., Capron, E., Carlson, A.E., Dutton, A., Fischer, H., Goelzer, H., Govin,
599 A., Haywood, A., Joos, F., Legrande, A.N., Lipscomb, W.H., Lohmann, G., Mahowald,
600 N., Nehrass-Ahles, C., Pausata, F.S.R., Peterschmidt, J.-Y., Phipps, S.J., Renssen, R.,
601 and Zhang, Q.: The PMIP4 contribution to CMIP6 – Part 2: Two interglacials, scientific
602 objective and experimental design for Holocene and Last Interglacial simulations,
603 *Geosci. Model Dev.*, 10, 3979–4003, <https://doi.org/10.5194/gmd-10-1-2017>, 2017
- 604 Piao, S., Friedlingstein, P., Ciais, P., Zhou, L., and Chen, A.: Effect of climate and CO₂ changes
605 on the greening of the Northern Hemisphere over the past two decades. *Geophys. Res.*
606 *Lett.* 33, L23402, <https://doi.org/10.1029/2006GL028205>, 2006.
- 607 Piao, S., Wang, X., Park, T., Chen, C., Lian, X., He, Y., Bjerke, J. W., Chen, A., Ciais, P.,
608 Tømmervik, H., Nemani, R. R., and Myneni, R. B.: Characteristics, drivers and
609 feedbacks of global greening, *Nature Rev. Earth Environ.*, 1, 14–27.
610 <https://doi.org/10.1038/s43017-019-0001-x>, 2020.
- 611 Peng, Y., Bloomfield, K.J., and Prentice, I.C.: A theory of plant function helps to explain leaf-
612 trait and productivity responses to elevation, *New Phytol.*, 226, 1274–1284, 2020.
- 613 Pickett, E.J., Harrison, S.P., Hope, G., Harle, K., Dodson, J.R., Kershaw, A.P., Prentice, I.C.,
614 Backhouse, J., Colhoun, E.A., D’Costa, D., Flenley, J., Grindrod, J., Haberle, S.,
615 Hassell, C., Kenyon, C., Macphail, M., Martin, H., Martin, A.H., McKenzie, M.,
616 Newsome, J.C., Penny, D., Powell, J., Raine, J.I., Southern, W., Stevenson, J., Sutra,
617 J.P., Thomas, I., van der Kaars, S., and Ward, J.: Pollen-based reconstructions of biome
618 distributions for Australia, Southeast Asia and the Pacific (SEAPAC region) at 0, 6000
619 and 18,000 ¹⁴C yr B.P. *Journal of Biogeography* 31: 1381–1444, [10.1111/j.1365-2699.2004.01001.x](https://doi.org/10.1111/j.1365-2699.2004.01001.x), 2004.
- 621 Polley, H.W., Johnson, H.B., Marino, B.D., and Mayeux, H.S.: Increases in C₃ plant water-use
622 efficiency and biomass over glacial to present CO₂ concentrations, *Nature*, 361, 61–64,
623 1993.
- 624 Prentice, I.C., Dong, N., Gleason, S.M., Maire, V., Wright, I.J.: Balancing the costs of carbon
625 gain and water transport: testing a new theoretical framework for plant functional
626 ecology, *Ecol. Lett.*, 17, 82–91, 2014.
- 627 Prentice, I.C., Harrison, S.P., and Bartlein P.J.: Global vegetation and terrestrial carbon cycle
628 changes after the last ice age, *New Phytol.*, 189, 988–998, 2011.
- 629 Prentice, I.C., Jolly, D., and BIOME 6000 Participants, 2000. Mid-Holocene and glacial-
630 maximum vegetation geography of the northern continents and Africa, *J. Biogeog.*, 27:
631 507–519.
- 632 Prentice, I.C., Kelley, D.I., Foster, P.N., Friedlingstein, P., Harrison S.P., and Bartlein P.J.:
633 Modeling fire and the terrestrial carbon balance, *Glob. Biogeochem. Cycl.*, 25,
634 GB3005, [doi:10.1029/2010GB003906](https://doi.org/10.1029/2010GB003906), 2011.



- 635 Rommerskirchen, F., Eglinton, G., Dupont, L., and Rullkötter, J.: Glacial/interglacial changes
636 in southern Africa: Compound-specific $\delta^{13}\text{C}$ land plant biomarker and pollen records
637 from southeast Atlantic continental margin sediments, *Geochem. Geophys. Geosy.*, 7,
638 Q08010, 2006.
- 639 Sato, H., Kelley, D.I., Mayor, S.J., Martin Calvo, M., Cowling, S.A., and Prentice, I.C.: Dry
640 corridors opened by fire and low CO_2 in Amazonian rainforest during the Last Glacial
641 Maximum, *Nat. Geosci.*, 14, 578–585, <https://doi.org/10.1038/s41561-021-00777-2>,
642 2021.
- 643 Sinninghe Damsté, J. S., Verschuren, D., Ossebaar, J., Blokker, J., van Houten, R., Plessen,
644 B., and Schouten, S.: A 25,000-year record of climate-induced changes in lowland
645 vegetation of eastern equatorial Africa revealed by the stable carbon-isotopic
646 composition of fossil plant leaf waxes, *Earth Planet. Sci. Lett.*, 302, 236–246, 2011.
- 647 Smith, N.G., and Keenan, T.F.: Mechanisms underlying leaf photosynthetic acclimation to
648 warming and elevated CO_2 as inferred from least-cost optimality theory, *Glob.*
649 *Change Biol.*, 26, 5202–5216, 2020.
- 650 Smith, N.G., Keenan, T.F., Prentice, I.C., Wang, H., Wright, I.J., Niinemets, U, Crous, Y.,
651 Domingues, T.F., Guerrieri, R., Ishida, F.Y., Kattge, J., Kruger, E.L., Maire, V.,
652 Rogers, A., Serbin, S.P., Tarvainen, L., Togashi, H.F., Townsend, P.A., Wang, M.,
653 Weerasinghe, L.K., and Zhou, S-X.: Global photosynthetic capacity is optimized to
654 the environment, *Ecol. Lett.*, 22, 506–517, 2019.
- 655 Stein, U., and Alpert, P.: Factor separation in numerical simulations, *J. Atmos. Sci.*, 50, 2107–
656 2115, 1993.
- 657 Stocker, B.D., Wang, H., Smith, N.G., Harrison, S.P., Keenan, T., Sandoval, D., Davis, T., and
658 Prentice, I.C.: P-model v1.0: an optimality-based light use efficiency model for
659 terrestrial gross primary production, *Geosci. Model Devel.*, 13, 1545–1581, 2020.
- 660 Swinehart, D.F.: The Beer-Lambert Law, *J. Chem. Educ.*, 39, 333,
661 <https://doi.org/10.1021/ed039p333>, 1962.
- 662 Vogts, A., Schefuß, E., Badewien, T., and Rullkötter, J.: n-alkane parameters derived from a
663 deep-sea sediment transect off south-west Africa reflect continental vegetation and
664 climate conditions, *Org. Geochem.*, 47, 109–119, 2012.
- 665 Wang, H., Prentice, I.C., Cornwell, W.M., Keenan, T.F., Davis, T.W., Wright, I.J., Evans, B.J.,
666 and Peng, C.: Towards a universal model for carbon dioxide uptake by plants. *Nature*
667 *Plants*, 3, 734–741, 2017.
- 668 Williams, I.N., and Torn, M.S.: Vegetation controls on surface heat flux partitioning, and
669 land-atmosphere coupling, *Geophys. Res. Lett.*, 42, 9416–9424,
670 [doi:10.1002/2015GL066305](https://doi.org/10.1002/2015GL066305), 2015.
- 671 Williams, J.W.: Variations in tree cover in North America since the last glacial maximum, *Glob.*
672 *Planet. Change*, 35, 1-23, [https://doi.org/10.1016/S0921-8181\(02\)00088-7](https://doi.org/10.1016/S0921-8181(02)00088-7), 2003.
- 673 Wohlfahrt, J., Harrison, S.P., Braconnot, P., Hewitt, C.D., Kutzbach, J.E., Kitoh, A.,
674 Mikolajewicz, U., Otto-Bliesner, B., and Weber, N.: Evaluation of coupled ocean-
675 atmosphere simulations of northern hemisphere extratropical climates in the mid-
676 Holocene, *Clim. Dyn.*, 31, 871–890, [10.1007/s00382-008-0415-5](https://doi.org/10.1007/s00382-008-0415-5), 2008.
- 677 Yang, J-W., Brandon, M., Landais, A., Duchamp-Alphonse, S., Blunier, T., Prie, F., and
678 Extier, T.: Global biosphere primary productivity changes during the past eight glacial
679 cycles, *Science*, 375, 1145–115, [10.1126/science.abj8826](https://doi.org/10.1126/science.abj8826), 2022.
- 680 Zeng, Z., Piao, S., Li, L. Zhou, L., Ciais, P., Wang, T., Li, Y., Lian, X., Wood, E. F.,
681 Friedlingstein, P., Mao, J., Estes, L.D., Myneni, R.B., Peng, S., Shi, X., Seneviratne,
682 S.I., and Wang, Y.: Climate mitigation from vegetation biophysical feedbacks during
683 the past three decades, *Nature Clim. Change*, 7, 432–436, <https://doi.org/10.1038/nclimate3299>, 2017.
- 684



685 Zhou, B., Cai, W., Zhu, Z., Wang, H., Harrison, S.P., and Prentice, I.C.: A general model for
686 the seasonal to decadal dynamics of leaf area, bioRxiv,
687 <https://www.biorxiv.org/content/10.1101/2024.10.23.619947v1>, 2024.
688 Zhu, Z., Wang, H., Harrison, S.P., Prentice, I.C., Qiao, S., and Tan, S.: Optimality principles
689 explaining divergent responses of alpine vegetation to environmental change, Glob.
690 Change Biol., 29, 126-142, doi: 10.1111/gcb.16459, 2022.